nature cell biology

Monoubiquitinated H2B is associated with the transcribed region of highly expressed genes in human cells

Neri Minsky[1,3], Efrat Shema[1], Yair Field[2], Meromit Schuster[2], Eran Segal[2] and Moshe Oren[1,4]

Histone modifications have emerged as important regulators of transcription[1,2]. Histone H2B monoubiquitination has also been implicated in transcription[3,4]; however, better understanding of the biological significance of this modification in mammalian cells has been hindered by the lack of suitable reagents, particularly antibodies capable of specifically recognizing ubiquitinated H2B (ubH2B). Here, we report the generation of anti-ubH2B monoclonal antibodies using a branched peptide as immunogen. These antibodies provide a powerful tool for exploring the biochemical functions of H2B monoubiquitination at both a genome-wide and gene-specific level. Application of these antibodies in high resolution chromatin immunoprecipitation (ChIP)-chip experiments in human cells, using tiling arrays, revealed preferential association of ubiquitinated H2B with the transcribed regions of highly expressed genes. Unlike dimethylated H3K4, ubH2B was not associated with distal promoter regions. Furthermore, experimental modulation of the transcriptional activity of the tumour suppressor p53 was accompanied by rapid changes in the H2B ubiquitination status of its *p21* target gene, attesting to the dynamic nature of this process. It has recently been demonstrated that the apparent extent of gene expression often reflects elongation rather than initiation rates[5]; thus, our findings suggest that H2B ubiquitination is intimately linked with global transcriptional elongation in mammalian cells.

A link between histone H2B monoubiquitination and transcription was proposed over a decade ago[6]. More recent studies, using yeast cells, reveal a complex relationship between H2B ubiquitination and transcriptional control: although H2B ubiquitination has been implicated in transcriptional silencing[7–10], other studies suggest a positive role for this modification in transcriptional initiation and elongation[11–15].

In yeast, functional analysis was greatly aided by the construction of strains carrying a point mutation in the ubiquitination site of the single H2B protein[11,14–16]. This strategy cannot be implemented in mammalian cells, whose genomes carry numerous *H2B* genes[17]. Furthermore, nucleotide sequence differences between individual *H2B* genes severely hinder the use of short interfering RNA (siRNA) to knockdown endogenous *H2B* in mammalian cells. These obstacles can be partially circumvented by using cell-free transcription systems and this approach revealed a cooperation between H2B monoubiquitination and the histone chaperone FACT in regulating elongation by RNA polymerase II (ref. 18). Nevertheless, there remains an acute lack of definitive information on H2B monoubiquitination in living mammalian cells.

Deciphering the role of mammalian H2B ubiquitination could be greatly facilitated by antibodies specific to ubH2B. However, unlike other histone covalent modifications, the ubiquitin moiety is a 76 amino-acid polypeptide that cannot be comprised within the specificity-determining region of an antibody. To overcome this impediment, mice were immunized with a branched peptide (Fig. 1a) corresponding to the conjugation site of ubiquitin on human histone H2B[19]. Several ubH2B-specific hybridomas were obtained, and one was selected for further use. When reacted with a whole cell extract (WCE) or acid extract of human U2OS cells, this antibody specifically recognized a single band migrating at the position of ubH2B (Fig. 1b) with no detectable cross reactivity with either non-ubiquitinated H2B or ubH2A. This was further confirmed by the use of purified calf thymus histone H2A or histone H2B, in addition to the acid-extract fraction from HEK293 cells (see Supplementary Information, Fig. S1). Moreover, the antibody identified its target in extracts of cells transfected with wild-type human H2B, but not with H2B mutated at Lys 120, which can not undergo monoubiquitination (Fig. 1c). Notably, the same band was also seen, albeit faintly, with an anti-ubiquitin antibody. *Saccharomyces cerevisiae* ubH2B was not recognized efficiently (data not shown).

[1]Department of Molecular Cell Biology, The Weizmann Institute of Science, Rehovot 76100, Israel. [2]Department of Computer Science and Applied Mathematics, The Weizmann Institute of Science, Rehovot 76100, Israel. [3]Current address: Laboratory of Biochemistry and Molecular Biology, The Rockefeller University, New York, NY 10021, USA.
[4]Correspondence should be addressed to M.O. (e-mail: moshe.oren@weizmann.ac.il)

Received 3 December 2007; accepted 8 January 2008; published online 16 March 2008; DOI: 10.1038/ncb1712

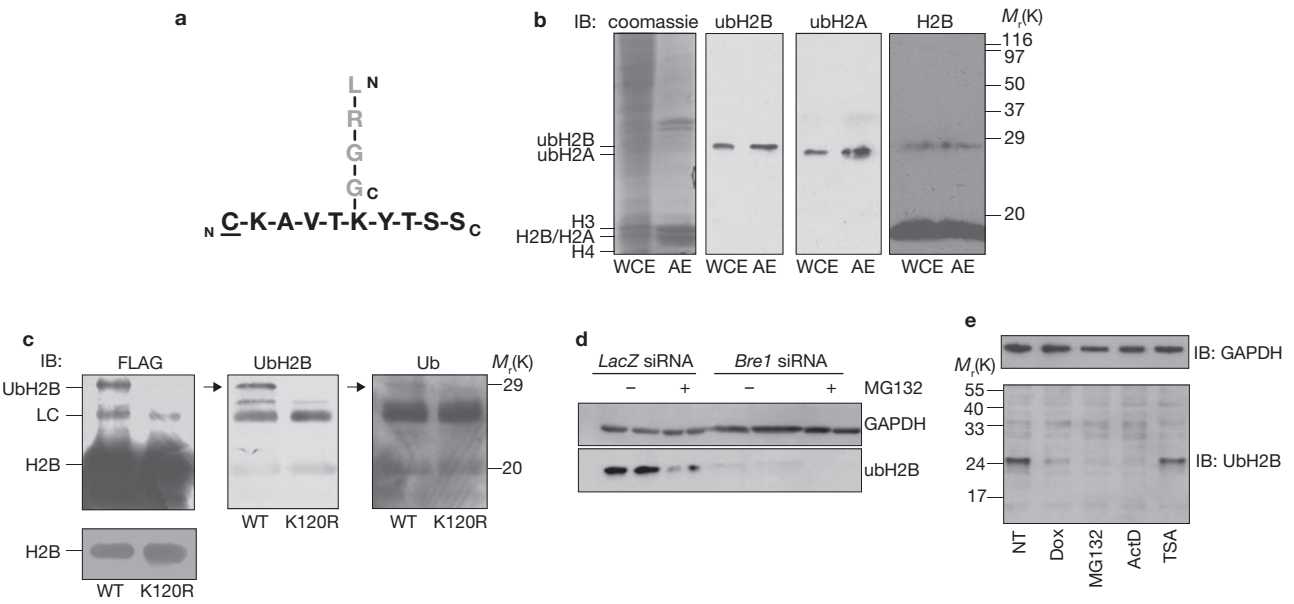

Figure 1 Generation and validation of anti-ubH2B antibodies. (**a**) Branched peptide used for immunization. The amino acid sequences in black and grey are derived from H2B and ubiquitin, respectively. (**b**) Whole cell extract (WCE) or acid extracted proteins (AE) from HEK-293T cells were subjected to SDS–PAGE followed by Coomassie staining or western blot (IB) analysis with the indicated antibodies. ubH2B and ubH2A indicate for monoubiquitinated H2B and H2A, respectively. Positions of modified and non-modified histones are indicated. (**c**) HEK-293T cells were transfected with either wild-type (WT) FLAG-tagged H2B or a ubiquitination-deficient Flag-tagged H2B mutant (K120R). After 48 h, denatured cell extracts were subjected to immunoprecipitation with anti-Flag antibody. Pellets were resolved by SDS–PAGE followed by western blot analysis with the antibodies indicated above each panel. The lower left panel represents a short exposure of the upper panel. Positions of monoubiquitinated and non-modified Flag-H2B are indicated. LC, antibody light chain. Uncropped images of the western blot scans are shown in the Supplementary Information, Fig. S2. (**d**) U2OS cells were transfected in duplicate with *hBre1* siRNA or *LacZ* siRNA as control, and then either treated with MG132 (12.5 μM, 30 min) or left untreated. Cell extract aliquots containing equal amounts of total protein were subjected to western blot analysis with the anti-ubH2B antibody. GAPDH was used as a loading control. Each pair represents duplicate dishes. Uncropped images of the western blot scans are shown in the Supplementary Information, Fig. S2. (**e**) U2OS cells were treated with doxorubicin (Dox, 1 μM, 14 h), MG132 (25 μM, 2 h), actinomycin D (ActD, 5 μg ml^{-1}, 4 h) and trichostatin A (TSA, 100 ng ml^{-1}, 14 h), or left untreated (NT). Cell extracts were subjected to western blot analysis with the anti-ubH2B antibody. GAPDH was used as a loading control.

hBre1/RNF20 is the major H2B-specific E3 ubiquitin ligase in mammalian cells[20]. As observed in Fig. 1d, siRNA-mediated knockdown of endogenous *hBre1* greatly reduced the intensity of the signal obtained with the anti-ubH2B antibody; the amount of residual signal varied in different cell lines, and was generally inversely correlated with the efficacy of *hBre1* knockdown (data not shown). This argues strongly in favour of the specificity of the antibody.

To our knowledge, although an attempt to generate polyclonal antibodies against ubH2A has been described[21], and a monoclonal antibody against ubH2A was generated serendipitously by immunization with nuclear pellets[22], these are the first monoclonal antibodies generated intentionally to target a specific ubiquitin conjugate.

The utility of the antibodies was further validated by analysis of U2OS human osteosarcoma cells subjected to a variety of agents that modulate ubH2B levels. In agreement with earlier reports, a proteasome inhibitor[23] (MG132; Fig. 1d, e), and the transcriptional inhibitor actinomycin D[3] (ActD; Fig. 1e) depleted ubH2B efficiently; the effect of MG132 was remarkably rapid (Fig. 1d). DNA damage was also suggested to reduce ubH2B levels[24], and treatment with doxorubicin (Dox) caused a marked drop in ubH2B, whereas the histone deacetylase inhibitor trichostatin A (TSA) had little or no effect.

The availability of ubH2B-specific monoclonal antibodies facilitates, for the first time, a definitive genome-wide analysis of H2B ubiquitination patterns through the use of a ChIP-microarray strategy (ChIP-chip). To that end, chromatin was immunoprecipitated from human colorectal carcinoma HCT116 cells with the ubH2B antibody. A parallel reaction was performed with antibodies specific for Lys 4-dimethylated histone H3 (H3K4me2), as previous studies suggested that ubH2B is a prerequisite for H3K4 methylation in yeast[10,25]. Following amplification and labelling, the resultant DNA was hybridized with a human promoter 1.0R high-resolution tiling array, which offered an extensive 10 kb coverage of approximately 7.5 kb upstream through 2.45 kb downstream to the 5′ transcription start site (TSS) for approximately 25,000 human genes. To control for histone density, parallel ChIP-chip was performed for histone H3 and signals obtained for either ubH2B or H3K4me2 were normalized to the corresponding H3 signal. The data represents an average of two arrays for each ChIP (Fig. 2).

To explore relationships between H2B ubiquitination and transcriptional activity, RNA from parallel HCT116 cultures was used in standard expression microarray analysis. A total of 16,101 genes, for which there was acceptable information on expression, TSS position and modification status along the probed genomic region, were considered for further analysis. The correlation between expression level and the extent of a particular modification (ubH2B or H3K4me2, normalized for H3 and averaged over a 500 bp window) was calculated for the entire group of genes, at various positions along the probed region. ubH2B levels were significantly positively correlated with gene expression in the region starting near the TSS and extending into the

transcribed region, with a gradual increase further into the transcribed region (Fig. 2a). Within the resolution of the ChIP method, which employs genomic DNA fragments of approximately 500 bp in length, there was no significant association between expression and H2B ubiquitination in the region upstream to the TSS. Unlike ubH2B, the presence of H3K4me2 correlated with expression over a large region spanning the TSS, with the strongest correlations observed at approximately 1 kb upstream of the TSS and 1 kb downstream of it (Fig. 2a); this bimodal distribution is consistent with earlier data[19]. Thus, whereas H3K4 dimethylation on the promoter region (defined as upstream to the TSS) is clearly associated with expression, this is not the case for UbH2B. Although we can not exclude the possibility that H2B ubiquitination may spill into the first few nucleosomes preceding the TSS of some expressed genes, our data clearly shows that this modification is preferentially targeted to within the transcribed region.

The above analysis showed that each modification had a different signature over the TSS region that correlates with expression. We therefore calculated an expression signature score for each gene that averages the signals along the TSS region, with weights proportional to the particular modification's regional correlation profile (shown in Fig. 2a). These signatures showed much higher correlation with expression than any individual position in the TSS region examined, with a correlation of 0.3 for H2B ubiquitination and a correlation of 0.6 for H3K4 dimethylation. To further interrogate the relationships between ubH2B and H3K4me2 in the context of gene expression, the 1000 most highly expressed genes and the 1000 least expressed genes, as deduced from the expression microarray analysis, were plotted along the two-dimensional space of the ubH2B expression signature and H3K4me2 expression signature. ubH2B and H3K4me2 expression signatures were significantly correlated with each other and with gene expression levels: 82.4% of the highly expressed genes had both marks together, whereas 47.4% of the least expressed genes had neither modification (Fig. 2b). Furthermore, in agreement with the data in Fig. 2a, most ubH2B-positive genes (71.7%) were highly expressed, whereas most ubH2B-low genes (76.4%) were not expressed. Interestingly, within the group of ubH2B-positive genes that nevertheless failed to express, many (54.5%) did not carry the H3K4me2 signature, probably accounting for their inefficient transcription. It is also noteworthy that although H2B ubiquitination and H3K4 dimethylation correlated well downstream of the TSS, this correlation did not extend into the upstream region, where H2B ubiquitination was far less pronounced than H3K4 dimethylation (Fig. 2a). This suggests that H3K4 dimethylation downstream of the TSS and upstream of it may be governed by different mechanisms, with only the former being coupled to H2B ubiquitination.

The predictions made on the basis of the global data analysis were next validated for individual representative genes. ChIP was performed with antibodies specific for either ubH2B or total H2B, with and without partial *hBre1* knockdown (Fig.3), followed by real-time PCR using primer sets against different genomic regions (see Supplementary Information, Methods). The analysis included three highly expressed genes and three very lowly expressed/non-expressed genes, and ubH2B signals were normalized for the corresponding total H2B signal. Consistent with the genome-wide ChIP-chip data, ubH2B was found to be preferentially associated with the transcribed region of highly expressed but not lowly expressed genes (Fig. 3a). As expected, suppressing *hBre1* expression markedly reduced the extent of associated ubH2B in all cases. Notably,

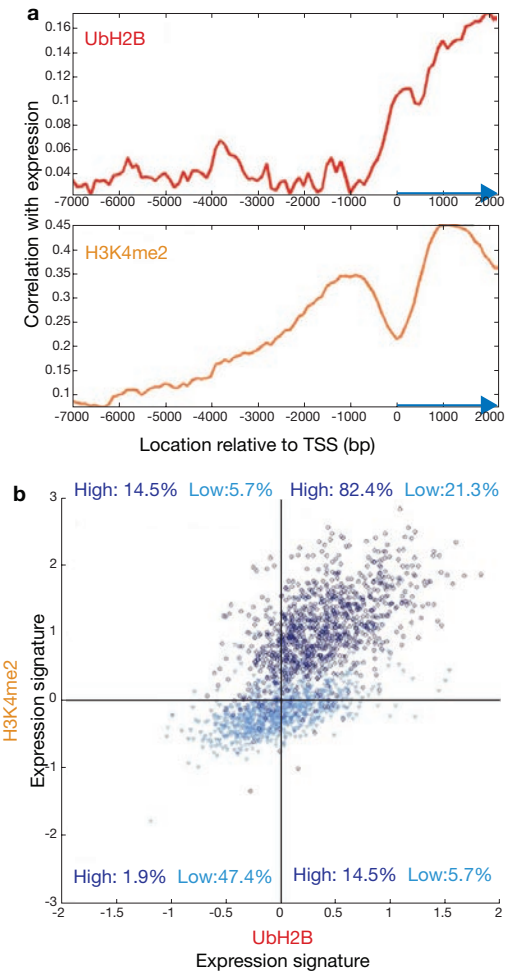

Figure 2 Analysis of ubH2B and H3K4me2 patterns around transcription start sites. (**a**) Correlation of ubH2B levels with gene expression across different regions around the TSS. For 16,101 genes, the Pearson correlation between the expression level of the genes and their ubH2B or H3K4me2 levels at various positions along the probed region was calculated. (**b**) A score for the modification expression signature (ubH2B and H3K4me2) was calculated for each gene as a weighted average of the signals along the region around the TSS, with weights given proportionately to the regional correlation profile. Thus, the expression signature of ubH2B is dominated by the signal over the transcribed region, whereas the expression signature of H3K4me2 is dominated by the signals over the entire region, giving most weight to the two peaks 1 kb upstream and 1 kb downstream of the TSS. The 1000 most highly expressed and 1000 least expressed genes (dark blue circles and light blue triangles, respectively) were plotted individually for their ubH2B and H3K4me2 expression signatures.

the upstream regions of the highly expressed genes, presumably containing distal promoter elements, exhibited much lower ubH2B association; nevertheless, there still was some H2B ubiquitination in those regions and within the lowly expressed genes, as *hBre1* knockdown caused a further decrease in signal intensity in both cases (Fig. 3a).

The genome-wide ChIP-chip data addressed only the 5′ part of the transcribed regions. Therfore, a representative expressed gene, the p53-regulated *p21* gene, was subjected to more detailed ubH2B distribution analysis using primer sets spanning the entire gene and its upstream and downstream flanks (Fig. 3b). As seen in Fig. 3c, substantial H2B ubiquitination was observed throughout most of the transcribed region, becoming attenuated towards the end of that region (primer set EN).

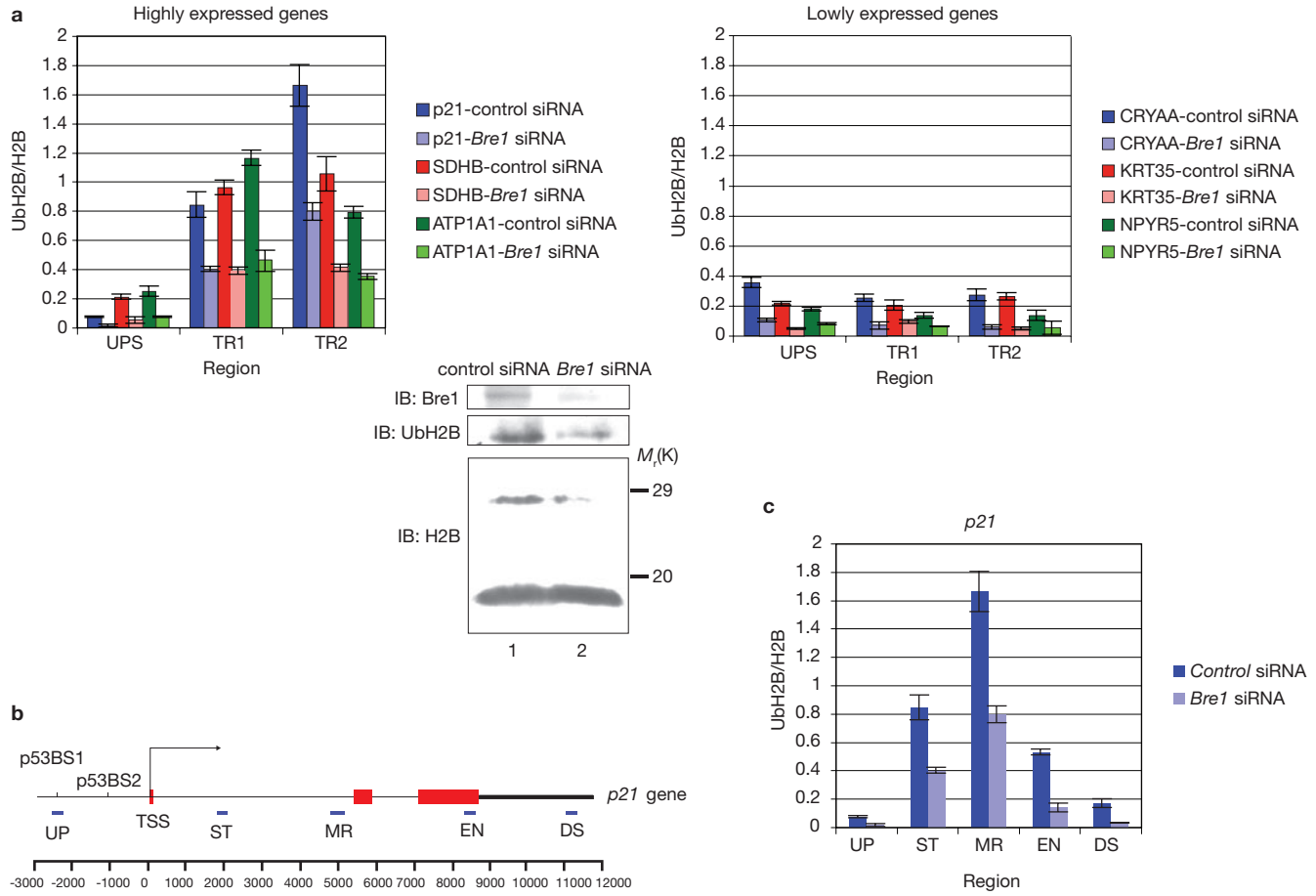

Figure 3 ubH2B is associated with the transcribed region of highly expressed genes. (**a**) HCT116 cells were transfected with either control siRNA or *hBre1* siRNA. After 96 h, cells were subjected to ChIP with anti-ubH2B antibody. Precipitated DNA was subjected to real-time qPCR analysis with primer pairs corresponding to the upstream region (UPS) or to two different locations within the transcribed regions (TR1 and TR2) of the indicated genes. The analysis was performed in parallel for selected highly expressed and lowly expressed genes. For each primer pair, ubH2B ChIP values were normalized to the corresponding total H2B ChIP. Western blot analysis of whole cell extracts from parallel cultures of the same experiment, probed for hBre1, UbH2B and total H2B is also shown. Error bars represent the s.d. values from four repetitions. (**b**) Schematic representation of the human *p21* gene. Positions of the two p53 binding sites (p53BS) within the promoter, TSS, exons (red) and primer pairs used for the real-time PCR analysis are indicated. UP, derived from the promoter, spans p53BS1 and is identical to *p21* UPS in **a**; ST corresponds to *p21* TR1 in **a**; MR is from the middle of the gene and corresponds to *p21* TR2 in **a**; EN and DS are derived from the end of the transcribed region and the region downstream to the *p21* gene, respectively. (**c**) The precipitated DNA described in **a** was subjected to real-time qPCR analysis with primer pairs corresponding to various regions of the *p21* gene (see **b**).

In contrast, ubH2B was not significantly associated with either the upstream region, encompassing the major p53 binding site (p53BS1) of the *p21* promoter, or the non-transcribed downstream region.

The data presented thus far provide a steady-state picture of H2B ubiquitination. To explore the dynamics of this process, we took advantage of H1299-tsp53 cells harbouring a temperature-sensitive p53 mutant. In these cells, p53 can be activated on shift to 32°C, leading to a time-dependent increase in the transcription of p53 target genes, including *p21* (ref. 26). Activation of p53 by shift to 32°C resulted in a gradual increase in ubH2B association with the transcribed region of the *p21* gene (Fig. 4). Remarkably, the increase in H2B ubiquitination coincided with the recruitment of PolII and preceded the accumulation of *p21* mRNA, suggesting an intimate association of ubH2B with the transcription process. Notably, on shifting the cells back to 37°C, ubH2B association with the transcribed region decreased rapidly, presumably via rapid deubiquitination, concomitantly with the dissociation of PolII. A similar behaviour was displayed by additional p53 target genes (data not shown). Thus, H2B ubiquitination is a very dynamic process, which can be turned on and off rapidly in concert with the formation of active transcription complexes.

Although H2B ubiquitination in mammalian cells had already been reported more than 25 years ago[27], its functional analysis has remained a formidable challenge, largely owing to the lack of suitable molecular tools. The new anti-ubH2B antibodies allow this challenge to be effectively addressed. They provide the opportunity to study gene-specific H2B ubiquitination in mammalian cells not exposed to any genetic manipulation or artificial protein overexpression, and should be equally applicable to samples obtained from human and animal tissues. The success of this strategy suggests that similar branched peptides may be used to generate other target-specific and site-specific ubiquitin-protein antibodies.

In summary, extending earlier observations in yeast[11,14,15], our findings imply that H2B ubiquitination is largely confined to the transcribed region of mammalian genes, and is closely correlated with active transcription. For most mammalian genes, ubH2B seems to be

excluded from the promoter, with the possible exception of promoter elements residing in very close proximity to the TSS. This observation is consistent with a coupling between H2B ubiquitination and the transcriptional elongation process. Interestingly, studies in yeast using anti-ubiquitin ChIP suggested association of ubH2B with promoters[6,8]. However, the primers used in these experiments were not designed to distinguish between ubH2B association with the promoter itself versus association with promoter-proximal sequences of the transcribed region. Thus, it is possible that, even in yeast, H2B ubiquitination does not spread deep into upstream promoter elements. Alternatively, the principles governing the distribution patterns of ubH2B may differ between yeast and mammals.

In agreement with yeast studies[11,15], we find that association of ubH2B with the transcribed region is very dynamic, being rapidly switched on or off depending on the transcriptional status of the gene. This implies that, in addition to H2B-specific E3 ligases (most notably hBre1/RNF20), efficient deubiquitylases must also constantly be at work to remove this mark — USP3 may be one example[28].

A recent study has revealed that although many promoters are constitutively active, many of the corresponding genes are transcribed inefficiently, owing to failed elongation[5]; thus, high expression rates often imply efficient transcriptional elongation. The preferential association of ubH2B with the transcribed regions of highly expressed genes therefore argues in favour of an intimate link between transcriptional elongation and H2B ubiquitination, while suggesting that this modification may not be implicated in transcriptional initiation in most mammalian genes. Nevertheless, although this represents the average pattern, numerous individual genes behave differently than the overall average (data not shown). It therefore remains likely that, beyond its genome-wide association with transcriptional elongation, mammalian H2B ubiquitination plays different unique roles in different gene contexts; for example, in some cases it may serve to mark genes for long-term activation[29] rather than being associated with the transcription process itself. Conversely, ubH2B may function in the transcriptional silencing of some genes. The ubH2B-specific antibodies now provide an opportunity to tackle these and many additional interesting possibilities. □

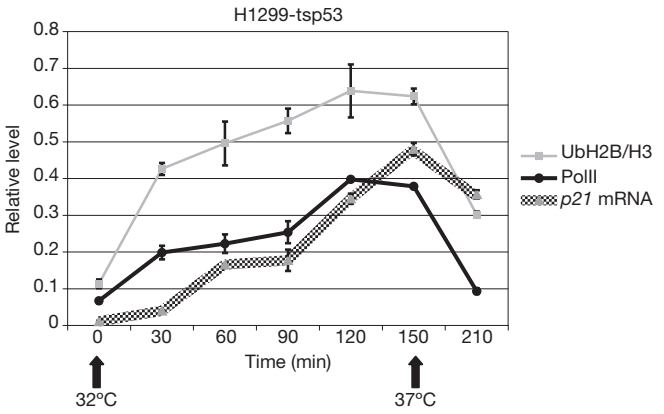

Figure 4 H2B ubiquitination of the *p21* gene correlates with p53-dependent transcriptional activation. (**a**) H1299-tsp53 cells, harbouring a temperature sensitive p53 mutant, were maintained at the restrictive temperature (37 °C), where p53 is inactive. At the time 0, cultures were shifted to the permissive temperature (32 °C), resulting in p53 activation. At 150 min, cultures were shifted back to 37 °C to turn off p53 transcriptional activity. At each indicated time point, cultures were subjected to ChIP with anti-ubH2B, anti-H3 or anti-RNA polymerase II (PolII) antibodies. The purified DNA from each reaction, along with the corresponding input sample, was subjected to real-time qPCR analysis with primers specific for the transcribed region of the *p21* gene (MR, Fig. 3b). Parallel cultures were subjected to total RNA extraction, followed by real-time RT–PCR analysis with primers corresponding to either *p21* mRNA or *GAPDH* mRNA. Squares represent ChIP analysis for ubH2B, normalized to H3 occupancy; circles represent PolII ChIP, normalized to input DNA; triangles represent relative *p21* mRNA levels after normalization for *GAPDH* mRNA in the same sample. Error bars represent the s.d. for four repetitions.

METHODS

Antibodies. The following commercial antibodies were used in this study: anti-H2B (ab1790, Abcam); anti-H3 (ab1791, Abcam); anti-ubH2A (05-679, Upstate); anti-H3K4me2 (07-030, Upstate). Anti-hBre1 antibodies and anti-ubiquitin polyclonal serum were kind gifts from R. G. Roeder (The Rockefellar University, New York, NY) and A. Ciechanover (The Technion, Haifa, Israel), respectively.

Peptide production. The branched peptide for immunization was synthesized by the solid phase method, using a multiple-peptide synthesizer AMS 422 (Abimed Analyzer-Technik Gmbh). The resulting peptide was HPLC-purified and characterized by MALDI-TOF mass spectroscopy and amino-terminal protein microsequencing. Before immunization, the peptide was conjugated with keyhole limpet hemocyanin (KLH).

Immunization. Four BALB/c mice (three-month old females) were injected subcutaneously with the conjugated preparations (50–100 μg) in complete Freund's adjuvant. Injections were repeated several times at intervals of two weeks. Three weeks later mice received two injections on two consecutive days.

Hybridoma fusion and growth. Three days after the last boost, spleens were removed and 100×10^6 cells from each individual spleen were fused with 20×10^6 NS0/1 myeloma cells. Fusion was carried out using 41% polyethylene glycol 1500 (Serva). Following fusion, cells were distributed into 96-well microplates at a concentration of 2×10^4 viable myeloma cells per well. Hybrid cells selected for growth in the presence of HAT were kept in a humidified incubator in the presence of 8% CO_2 in air. The cultures were maintained in high glucose DMEM (Gibco) supplemented with pyruvate (1 mM), glutamine (2 mM), penicillin (10 units ml^{-1}), streptomycin (20 μg ml^{-1}) and 15% heat inactivated horse serum (Biological Industries,). Positive hybrid cultures were weaned out of HAT, cloned and recloned by limiting dilutions, and propagated *in vitro* in large volumes of DMEM with horse serum.

Hybridoma screening by western blotting. U2OS whole cell extract was prepared and resolved by SDS–PAGE (15% polyacrylamide). Gels were electroblotted onto nitrocellulose membranes, blocked with 1% skimmed milk and individual strips were probed with hybridoma clone supernatants.

ChIP and DNA array hybridization. ChIP was performed essentially as described previously[30]. DNA amplification, labelling and array hybridization were carried out using the Affymetrix ChIP Assay kit according to the manufacturer's instructions.

Tiling array and expression data analysis. Genomic coordinates of probes were converted from human genome assembly hg16 to hg17 using the liftOver tool supplied by the UCSC genome browser. To normalize the data, the probes of each array were divided into bins according to their exact GC-content, and raw intensities in each bin were scaled to have zero median log intensity. Log ratios of sample to H3 control were then considered. TSS coordinates were taken from the UCSC genome browser and were profiled, for each gene, from 7000 bp upstream to 2300 bp downstream at 100 bp resolution, following a smoothing of 500 bp averaging window. For each coordinate in this TSS profile, the correlation between the modification signal (log-ratio) at that position and expression level was computed, yielding the regional correlation profiles in Fig. 2a. For each gene, and with respect to each modification, an expression signature score was computed by the cross product of the TSS profile and the normalized regional correlation profile (normalized over the sum of absolute values of all correlations in the profile). Gene expression values, taken as log of the maximum over probe

sets of the summarized expression value calculated using the RMA algorithm supplied by Affymetrix, were used to group genes by their relative extreme high and low expression in the analyzed profile set (1000 genes in each group).

RNA purification, reverse transcription and real-time PCR analysis. Total RNA was extracted with the NucleoSpin kit (Macherey). One microgram of each RNA sample was reverse transcribed with Moloney murine leukaemia virus reverse transcriptase (Promega) and random hexamer primers. Real-time quantitative PCR analysis of cDNA and genomic DNA was performed on an ABI 7000 machine (Applied Biosystems) with Syber Green PCR mastermix (Applied Biosystems). Primers for cDNA analysis were: *p21* mRNA forward, 5′GGCAGACCAGCATGACAGATT3′; *p21* mRNA reverse, 5′GCGGATTAGGGCTTCCTCTT3′, *GAPDH* mRNA forward, 5′ACCCACTCCTCCACCTTTGA3′; *GAPDH* mRNA reverse, 5′CTGTTGCTGTAGCCAAATTCGT3′. Primers for ChIP-qPCR are described in the Supplementary Information, Table S1.

Accession numbers. The microarry data has been deposited in NCBIs gene expression omnibus (GEO; http://www.ncbi.nlm.nih.gov/geo/) and is accessible through GEO series accession number GSE10453 (http://www.ncbi.nlm.nih.gov/geo/query/acc.cgi?acc=GSE10453).

Note: Supplementary Information is available on the Nature Cell Biology website.

ACKNOWLEDGMENTS
We are grateful to M. Fridkin for peptide design and synthesis, O. Leitner and A. Bren for immunizations and hybridoma fusion and growth, and S. Horn-Saban for DNA amplification and array hybridization. N.M. thanks R. Roeder for his support and encouragement. Supported in part by grant R37 CA40099 from the National Cancer Institute, a Prostate Cancer Foundation (Israel) Center of Excellence, the Dr. Miriam and Sheldon Adelson Medical Research Foundation, and the Yad Abraham Center for Cancer Diagnosis and Therapy.

AUTHOR CONTRIBUTIONS
N. M. and E, Sh. performed the experiments; Y. F. and M. S. performed he computational analysis; M. O. and E. Se. supervised the work. All authors contributed to the writing of the manuscript.

COMPETING FINANCIAL INTERESTS
The authors declare no competing financial interests.

Published online at http://www.nature.com/naturecellbiology/
Reprints and permissions information is available online at http://npg.nature.com/reprintsandpermissions

1. Berger, S. L. The complex language of chromatin regulation during transcription. *Nature* **447,** 407–412 (2007).
2. Kouzarides, T. Chromatin modifications and their function. *Cell* **128,** 693–705 (2007).
3. Osley, M. A. Regulation of histone H2A and H2B ubiquitylation. *Brief Funct. Genomic Proteomic* **5,** 179–189 (2006).
4. Shilatifard, A. Chromatin modifications by methylation and ubiquitination: implications in the regulation of gene expression. *Annu. Rev. Biochem.* **75,** 243–269 (2006).
5. Guenther, M. G., Levine, S. S., Boyer, L. A., Jaenisch, R. & Young, R. A. A chromatin landmark and transcription initiation at most promoters in human cells. *Cell* **130,** 77–88 (2007).
6. Davie, J. R. & Murphy, L. C. Inhibition of transcription selectively reduces the level of ubiquitinated histone H2B in chromatin. *Biochem. Biophys. Res. Commun.* **203,** 344–350 (1994).
7. Briggs, S. D. *et al.* Histone H3 lysine 4 methylation is mediated by Set1 and required for cell growth and rDNA silencing in *Saccharomyces cerevisiae*. *Genes Dev.* **15,** 3286–3295 (2001).
8. Lee, K. K., Florens, L., Swanson, S. K., Washburn, M. P. & Workman, J. L. The deubiquitylation activity of Ubp8 is dependent upon Sgf11 and its association with the SAGA complex. *Mol. Cell Biol.* **25,** 1173–1182 (2005).
9. Mutiu, A. I., Hoke, S. M., Genereaux, J., Liang, G. & Brandl, C. J. The role of histone ubiquitylation and deubiquitylation in gene expression as determined by the analysis of an HTB1(K123R) *Saccharomyces cerevisiae* strain. *Mol. Genet. Genomics* **277,** 491–506 (2007).
10. Sun, Z. W. & Allis, C. D. Ubiquitination of histone H2B regulates H3 methylation and gene silencing in yeast. *Nature* **418,** 104–108 (2002).
11. Henry, K. W. *et al.* Transcriptional activation via sequential histone H2B ubiquitylation and deubiquitylation, mediated by SAGA-associated Ubp8. *Genes Dev.* **17,** 2648–2663 (2003).
12. Shukla, A., Stanojevic, N., Duan, Z., Shadle, T. & Bhaumik, S.R. Functional analysis of H2B-Lys-123 ubiquitination in regulation of H3-Lys-4 methylation and recruitment of RNA polymerase II at the coding sequences of several active genes *in vivo*. *J. Biol. Chem.* **281,** 19045–19054 (2006).
13. Xiao, T. *et al.* Histone H2B ubiquitylation is associated with elongating RNA polymerase II. *Mol. Cell Biol.* **25,** 637–651 (2005).
14. Kao, C. F. *et al.* Rad6 plays a role in transcriptional activation through ubiquitylation of histone H2B. *Genes Dev.* **18,** 184–195 (2004).
15. Wyce, A. *et al.* H2B ubiquitylation acts as a barrier to Ctk1 nucleosomal recruitment prior to removal by Ubp8 within a SAGA-related complex. *Mol. Cell* **27,** 275–288 (2007).
16. Emre, N. C. *et al.* Maintenance of low histone ubiquitylation by Ubp10 correlates with telomere-proximal Sir2 association and gene silencing. *Mol. Cell* **17,** 585–594 (2005).
17. Marzluff, W. F., Gongidi, P., Woods, K. R., Jin, J. & Maltais, L. J. The human and mouse replication-dependent histone genes. *Genomics* **80,** 487–498 (2002).
18. Pavri, R. *et al.* Histone H2B monoubiquitination functions cooperatively with FACT to regulate elongation by RNA polymerase II. *Cell* **125,** 703–717 (2006).
19. Thorne, A. W., Sautiere, P., Briand, G. & Crane-Robinson, C. The structure of ubiquitinated histone H2B. *EMBO J.* **6,** 1005–1010 (1987).
20. Kim, J., Hake, S. B. & Roeder, R. G. The human homolog of yeast BRE1 functions as a transcriptional coactivator through direct activator interactions. *Mol. Cell* **20,** 759–770 (2005).
21. Plaue, S., Muller, S. & van Regenmortel, M. H. A branched, synthetic octapeptide of ubiquitinated histone H2A as target of autoantibodies. *J. Exp. Med.* **169,** 1607–1617 (1989).
22. Vassilev, A. P., Rasmussen, H. H., Christensen, E. I., Nielsen, S. & Celis, J. E. The levels of ubiquitinated histone H2A are highly upregulated in transformed human cells: partial colocalization of uH2A clusters and PCNA/cyclin foci in a fraction of cells in S-phase. *J. Cell Sci.* **108,** 1205–1215 (1995).
23. Mimnaugh, E. G., Chen, H. Y., Davie, J. R., Celis, J. E. & Neckers, L. Rapid deubiquitination of nucleosomal histones in human tumor cells caused by proteasome inhibitors and stress response inducers: effects on replication, transcription, translation, and the cellular stress response. *Biochemistry* **36,** 14418–14429 (1997).
24. Lis, E. T. & Romesberg, F. E. Role of Doa1 in the *Saccharomyces cerevisiae* DNA damage response. *Mol. Cell Biol.* **26,** 4122–4133 (2006).
25. Shahbazian, M. D., Zhang, K. & Grunstein, M. Histone H2B ubiquitylation controls processive methylation but not monomethylation by Dot1 and Set1. *Mol. Cell* **19,** 271–277 (2005).
26. Raver-Shapira, N. *et al.* Transcriptional activation of miR-34a contributes to p53-mediated apoptosis. *Mol. Cell* **26,** 731–743 (2007).
27. West, M. H. & Bonner, W. M. Histone 2B can be modified by the attachment of ubiquitin. *Nucleic Acids Res.* **8,** 4671–4680 (1980).
28. Nicassio, F. *et al.* Human USP3 is a chromatin modifier required for S phase progression and genome stability. *Curr. Biol.* **17,** 1972–1977 (2007).
29. Sridhar, V. V. *et al.* Control of DNA methylation and heterochromatic silencing by histone H2B deubiquitination. *Nature* **447,** 735–738 (2007).
30. Minsky, N. & Oren, M. The RING domain of Mdm2 mediates histone ubiquitylation and transcriptional repression. *Mol. Cell* **16,** 631–639 (2004).

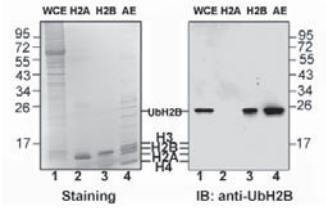

Figure S1 Western blot analysis with the anti-ubiquityl-H2B antibody (right panel) and Coomassie staining (left panel) of whole cell extract from U2OS cells (WCE, lane 1), purified histone H2A (lane 2), purified H2B (lane 3) and acid extracted proteins from HEK293 cells (AE, lane 4). Positions of non-modified histones and of uH2B are indicated.

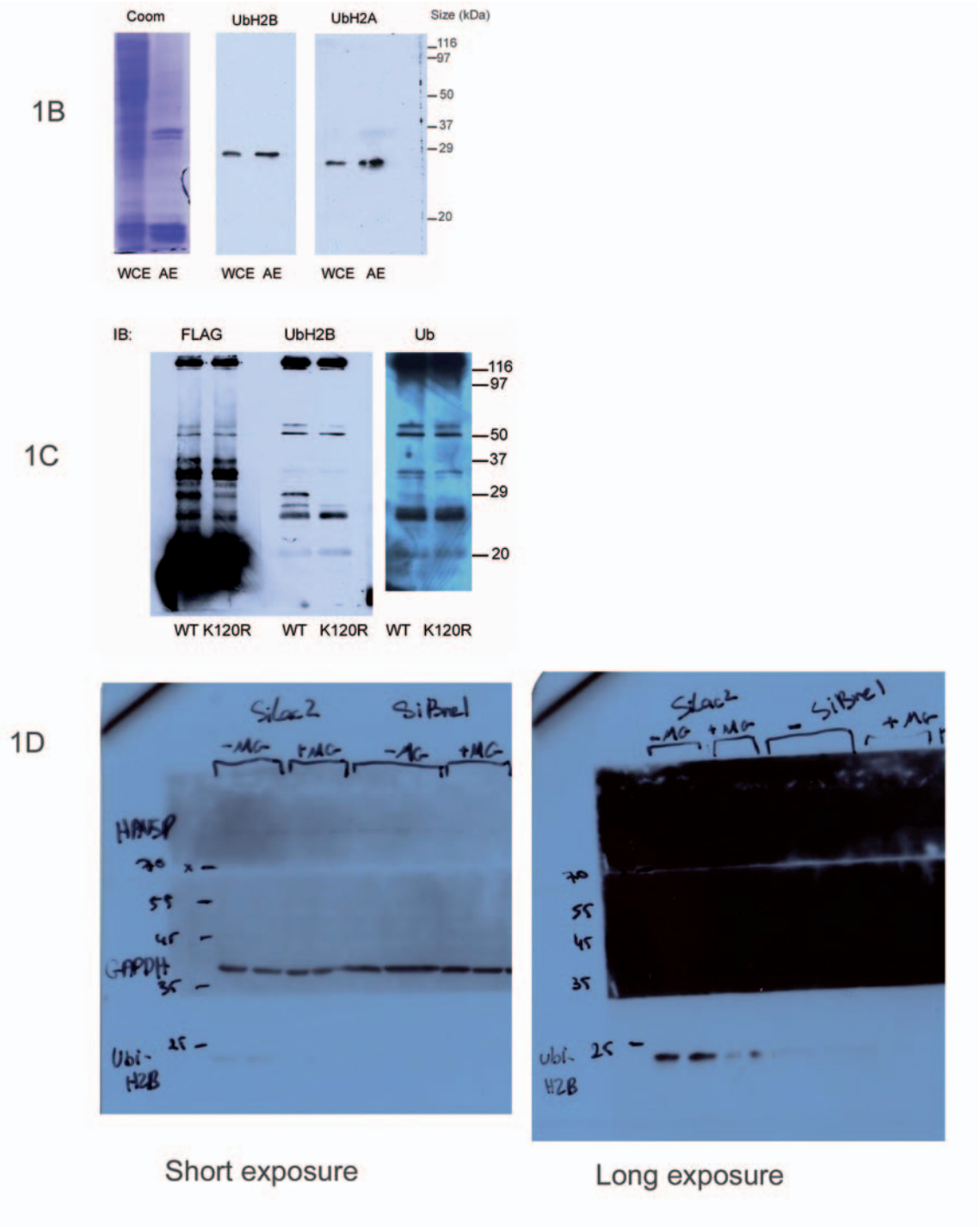

Figure S2 Full scans of key western data